Observation and characterization of a strained lateral superlattice in the oxidation of Ni(001)

R. S. Saiki, A. P. Kaduwela, J. Osterwalder,* and C. S. Fadley
Department of Chemistry, University of Hawaii at Manoa, 2545 The Mall, Honolulu, Hawaii 96822

C. R. Brundle
IBM Research Division, Almaden Research Center, 650 Harry Road, San Jose, California 95120-6099
(Received 2 November 1988)

The saturated oxide formed on Ni(001) under UHV conditions has been studied by x-ray photoelectron diffraction (XPD) and low-energy electron diffraction. At ambient temperature and with a 1200-L exposure to oxygen, the saturation oxygen coverage is found to be 4.3±0.4 monolayers (ML) as measured relative to the Ni(001) surface-atom density. [1 langmuir (L)$\equiv 10^{-6}$ Torr sec.] The oxide is furthermore found to grow primarily as NiO(001) in a highly strained superlattice for which the horizontal lattice constant is expanded by $\frac{1}{6}$ compared to the underlying Ni(001). The XPD results are found to be very sensitive to the degree of short-range order in the oxide before and after light annealing, particularly when obtained with high angular resolutions of approximately ±1.0°. Single-scattering calculations with spherical-wave scattering are found to give an excellent description of the XPD from the annealed and more-ordered overlayer. These results also suggest the general utility of high-resolution XPD for studying the degree of short-range positional order present in epitaxial overlayers.

INTRODUCTION

We report here the first observation of a strained lateral superlattice in the ambient-temperature oxidation of Ni(001). This study makes use of both high-energy x-ray photoelectron diffraction (XPD) and low-energy electron diffraction (LEED) to determine the structural characteristics of the oxide overlayer formed. Although the reaction of Ni(001) with oxygen has been the object of numerous studies,[1,2] no such superlattice has been discussed previously. A somewhat similar superlattice has been proposed in an early stage of the high-temperature oxidation of Ni(111) by Christensen *et al.*,[3] and we comment below on its relationship to the structure we observe. A prior XPD study by our group on O/Ni(001) has emphasized the structures formed at lower exposures.[4] We here will concentrate entirely on the saturated oxide of approximately 4 monolayers (ML) thickness which in this study was formed at ambient temperature with an oxygen exposure of 1200 langmuirs (L).[1] (1 L $\equiv 10^{-6}$ Torr sec.)

EXPERIMENTAL PROCEDURE AND SURFACE CHARACTERIZATION

The modified Hewlett-Packard 5950A system on which this combined LEED-XPD study was performed is discussed in detail elsewhere.[5] In addition, several azimuthal XPD scans of O 1*s* intensity were carried out at a very high angular resolution of ±1.5° in a VG Scientific ESCALAB5 system equipped with angle-defining tube arrays.[6] Surface cleanliness and oxide coverage were monitored by x-ray photoelectron spectroscopy (XPS) using standard core-intensity relationships for different surface overlayer morphologies.[5] Al $K\alpha$ radiation (1486.6 eV) was used for excitation in all spectra.

The saturated oxide thickness after a 1200-L exposure at ambient temperature and a pressure of 1.0×10^{-5} Torr was determined from the ratio of the O 1*s* intensity of the oxide to the Ni $2p_{3/2}$ intensity from the clean Ni surface just before the exposure. Both intensities were measured at a point well away from any strong photoelectron-diffraction features and chosen so as to represent averages over the XPD structure; doing such averaging has been shown to be crucial for deriving accurate overlayer coverages.[7] The intensity ratios so derived were found to be very reproducible, with values usually lying within ±5% of those used for deriving the coverages quoted here. The calculations incorporated full allowance for inelastic attenuation in the assumed uniform oxide overlayer, and also included the variation of analyzer solid angle with kinetic energy.[7] Theoretical relative differential photoelectric cross sections for O 1*s* and Ni $2p_{3/2}$ were used.[8] The electron mean free path in the oxide at the O 1*s* kinetic energy (954 eV) was taken to be 12.3 Å.[7] This analysis yields an oxide thickness equivalent to 4.3±0.4 ML of oxygen as measured with respect to the Ni(001) surface density of 1.61×10^{15} atoms/cm^2. (Most of the uncertainty here stems from that in the mean free paths used.) Neglecting overlayer attenuation yields a value of 2.4 ML and demonstrates the considerable importance of this correction. Upon annealing briefly to approximately 250 °C, the attenuation-corrected value drops to 2.0–3.0 ML, although this decrease was very sensitive to the time of annealing and not fully reproducible. Such a decrease could be due to oxygen diffusion into the bulk.[1] Also, a simple thickening of the oxide layer into islands leaving relatively low-exposure areas in between has been suggested previously[1,9] and would yield the same effect on our attenuation-

 ©1989 The American Physical Society

corrected numbers. This is because our analysis assumes a uniform overlayer, but in the case of thicker islands (yielding a patched overlayer) the oxygen at the bottom of each island would experience enhanced inelastic scattering. Thus, the total O 1*s* intensity would be lowered for thicker patched islands, and our effective coverage based on a uniform overlayer model would go down.

Our saturation coverages before annealing are thus significantly higher than the approximately 2 ML discussed in some prior studies in the literature.[1,9,10] In order to check our analysis procedure, we have used a well-defined point in the exposure-versus-coverage or kinetics curve that corresponds to the strongest region of the $c(2\times2)$O LEED pattern. This point is defined as the minimum-slope exposure along a short $c(2\times2)$ plateau in the kinetics curve; it is found to occur at 30–40 L in our experiment. Assuming in this case that there is no attenuation in the partial monolayer formed and using all other inputs to the calculation as for the oxide overlayer, we get a result of 0.37 ± 0.04 ML that is in excellent agreement with most prior studies.[1,2,9] [It should be noted that higher coverages for saturation $c(2\times2)$O can be achieved under different experimental conditions, such as exposing at 50–150 °C above room temperature[11] and/or using annealing and reexposing cycles.] Looking at our results in another way, the ratio of the O 1*s* intensity at saturation coverage to that at the $c(2\times2)$ reference point is found to be 6.63; this implies that the *minimum* coverage value at saturation (which would be calculated with neglect of overlayer attenuation) is $0.37\times6.6=2.4$ ML. Correcting this value for attenuation then yields the 4.3 ML that we finally derive. Previous XPS work on a different Ni(001) crystal and in a different laboratory[12] gave O 1*s* intensity ratios from saturation to $c(2\times2)$ that are fully compatible with the high-coverage values we are suggesting. Both sets of XPS data show well-defined $c(2\times2)$ plateaus in their kinetics curves centered at rather high exposures of 30–40 L; this indicates a low defect density and rules out the possibility that the high saturation coverage is a result of poor surface quality. Thus, these combined XPS results provide a fully-self-consistent picture and support a saturation coverage of about 4 ML at an exposure of 1200 L.

One possible source of the discrepancy between our results and others for saturation coverages is that several prior studies have found lower exposures in the 200-L range to yield saturation, whereas our crystal did not reach saturation until approximately 500–600 L. Another source is that prior electron spectroscopic studies may not have correctly allowed for the combined effects of both outgoing Auger-electron- or photoelectron-diffraction and overlayer attenuation. In support of this latter suggestion, we note that the x-ray fluorescence work of Mitchell *et al.*,[10] in which attenuation corrections in x-ray emission from the overlayer should not be a problem, yield an O 1*s* ratio between saturation and $c(2\times2)$ coverage of approximately 10. Using an average value from the literature for the $c(2\times2)$ of 0.37 ML, which also agrees with our value, then yields a saturation coverage of $10\times0.37=3.7$ ML, a value not very far below our own value of 4.3 ML. This fluorescence ratio *cannot* be consistent with a $c(2\times2)$ coverage of 0.4 ML and a saturation coverage of near 2 ML. We conclude, therefore, that the question of quantification of oxygen coverage at saturation conditions, generally accepted to be about 2 ML in the literature,[1,9,10] needs reassessing. This problem will be dealt with in more detail in a later paper. For the present work, it is only necessary to establish that our saturated oxide layers are significantly thicker than 2 ML.

RESULTS AND DISCUSSION

In Fig. 1 we show LEED photographs and corresponding sketches of the spot patterns observed at an incident-beam energy of 64 eV. In Fig. 1(a) we show the pattern observed after the usual 1200-L exposure at ambient temperature (approximately 293 K). Here, one sees the square array characteristic of the underlying Ni(001) substrate, which is partly overlapping with a very diffuse square array of smaller dimension which is thought to be due to NiO present in the (100) orientation.[1,9] Also evident is the weaker 12-spot ring, which has been suggested to be caused by two domains of NiO in the (111) orientation that are rotated 30° apart.[1,9] But beyond this we see a clear and fully reproducible splitting of the diffuse NiO(001) spots into a centered square, as shown schematically in the right-hand panel. Direct measurements from these and similar photographs obtained in another experimental system[12] yields the following geometric re-

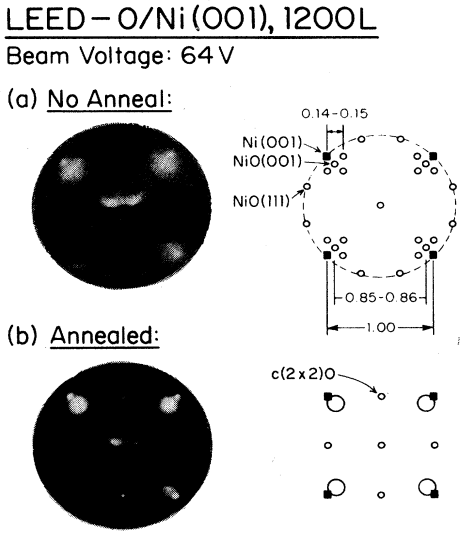

FIG. 1. (a) LEED spot pattern observed for ambient-temperature saturated oxide on Ni(001) at an incident energy of 64 eV. (The specimen holder obscures some spots from left to right across the image.) At right the positions and suggested origins of the several structures are indicated. (b) Same as (a), but after a light anneal to approximately 250 °C over about 10 min.

lationships among the spots.

(i) The centered square has an outside dimension along each edge that is very close to $\frac{1}{7}=14.3\%$ of that of the primary square array for Ni(001). The actual values are 14.3–15.1 % as measured from the photographs.

(ii) The first observation also implies that the primary square array for NiO(001) also has an outside dimension that is very close to $\frac{6}{7}=85.7\%$ of that of Ni(001), and this is found to be the case in direct measurement (84.9–85.7 %).

(iii) Both the 12-spot ring and the centered squares of NiO(001) yield spots that are coincident in position with the primary square array of Ni(001).

Upon annealing this ambient-temperature oxide to about 250 °C over a total of about 10 min, the spot patterns shown in Fig. 1(b) are found. As noted previously for this system,[1,9] the 12-spot ring disappears, the NiO(001) spots brighten, and there is also a very weak appearance of the same patterns seen with the $c(2\times2)$O overlayer formed at much lower exposures. We also note that the centered-square splitting of the NiO(001) spots is removed by this annealing.

Our suggested explanation for the extra spot splitting observed with the ambient-temperature oxide is that a lateral superlattice is formed due to the growth of reasonably large domains of strained NiO(001) whose NaCl lattice constant is on average exactly $\frac{1}{6}$ larger than that of the underlying Ni(001). The two arrays of Ni atoms that would be thus overlaid are shown in Figs. 2(a) and 2(b), and it is clear from the overlay in Fig. 2(c) that a new centered-square superlattice structure with dimensions that correspond to (6×6) NiO(001) units cells on (7×7) Ni(001) unit cells is formed. Thus, since the electrons in LEED will tend to penetrate several layers and scatter both singly and multiply, the regular beating of these two commensurate lattices could give rise to the additional spot splitting seen. A direct simulation of this effect with reduced photographic negatives of Figs. 2(a)–2(c) and a visible laser does indeed yield a spot splitting of the form and dimensions observed. The agreement between experiment and this optical simulation is furthermore best for an illuminated area of the negative of about (3×3) superlattice cells or about (18×18) NiO cells with overall dimensions of 74 Å×74 Å [that is, about the size of the arrays shown in Fig. 2(c)]; this provides a rough idea as to the possible domain sizes of the superlattices that may be involved.

Such a superlattice must be highly strained, however, since the positions of the Ni atoms in the NiO(001) structure can be totally in registry with those in the underlying Ni(001) only at the lighter centered-square positions that are obvious in Fig. 2(c), but must pass through regions of very strong mismatch in between these points. Two unit cells of this proposed structure (assuming for the moment only 2 ML of oxide with $\frac{1}{6}$ expansion) are shown in Fig. 3(a) for the case of perfect registry in one corner, and even for this case, the edge atoms in the two cells begin to be significantly out of registry. The true structure would no doubt relax in various ways to accommodate the strain induced, with one reasonable consequence being a net bowing outward over regions of the strongest mismatch. Such an effect might, in fact, be observable in a scanning-tunneling-microscope (STM) study of this system, although none has as yet been performed.

Additional information on the properties of this ambient-temperature oxide can be obtained from azimuthal- and polar-angle XPD scans for the O/Ni(001) system, an introduction to which appears elsewhere.[4] In Figs. 4 and 5, we show two additional sets of O 1*s* azimuthal data obtained at a very high angular resolution of ±1.5°. These data were obtained as full 360° scans which exhibited to a high degree the full C_{4v} point-group symmetry of the Ni(001) or NiO(001) surfaces and were then fourfold averaged into one quadrant. In Fig. 4 the polar angle of emission has been chosen to be as close as possible to 35.3°, implying that strong forward-scattering events due to Ni atoms may occur along ⟨111⟩ directions for emission from O atoms lying in the second and subse-

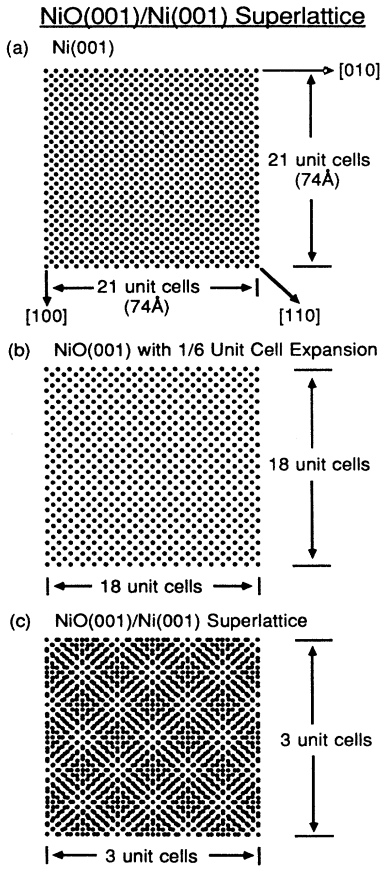

FIG. 2. (a) The array of Ni atoms on the surface of Ni(001), with various directions noted. (b) The Ni atoms in our proposed superlattice of NiO(001) with a $\frac{1}{6}=16.7\%$ lattice constant expansion with respect to the Ni. (c) An overlay of the two structures in (a) and (b) indicating the nature of the commensurate superlattice formed, as well as regions of both good registry (lighter color) and high mismatch and/or strain (darker color).

quent layers of the NiO(001) (see arrows in Fig. 3). Such strong diffraction peaks do indeed occur, as shown in the experimental curves for both the unannealed and annealed oxide at $\phi=45°$ in Fig. 4. The second case considered in Fig. 5 is a polar angle of 45°, which should and does yield strong peaks for O emitters in second and subsequent layers due to forward scattering from O atoms lying along ⟨110⟩ directions at $\phi=0°$ and 90° (see arrows in Fig. 3); again these strong features are seen for both the unannealed and annealed oxide.

Annealing the oxide overlayer as described previously causes significant changes in the XPD patterns seen at both polar angles, as shown in the bottom solid curves in Figs. 4 and 5. The dominant forward-scattering peaks are present in both cases, but there are significant changes in the relative intensities and positions of the additional features in these curves. In general, there is considerably more fine structure after the anneal, particularly for $\theta=45°$. This suggests that the oxide is more highly ordered, and perhaps thicker, after annealing. Thus, high-resolution XPD is shown to be sensitive to the subtle structural changes which have caused the LEED also to change between Figs. 1(a) and 1(b).

To get a better idea of how such changes might be linked to a reduction of the degree of strain and positional disorder present in the ambient-temperature oxide, we have carried out single-scattering cluster (SSC) calculations with spherical-wave scattering[5] for various possible oxide overlayer structures; these are shown as dashed curves in Figs. 4 and 5. The calculations shown at the

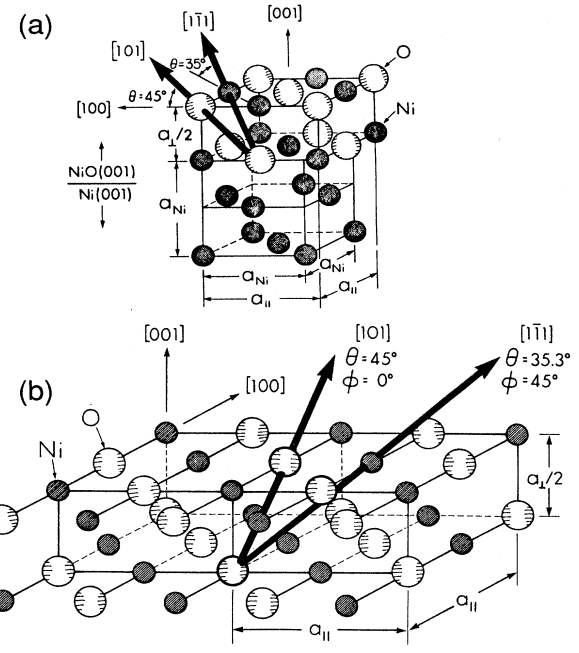

FIG. 3. (a) Two overlying unit cells from the superlattice in Fig. 2(c), with an assumed 2-ML thickness of NiO(001) and perfect registry at one corner. Also indicated are the two types of directions along which strong forward-scattering effects from near-neighbor atoms is expected, one for $\theta=35.3°$ (⟨111⟩ directions) and one for $\theta=45°$ (⟨110⟩ directions). (b) Two types of clusters used to simulate the reduction of long-range order in the strained superlattice: a 35-atom cluster over about two unit cells, and a minimal five-atom cluster (atoms shown in heavier outline).

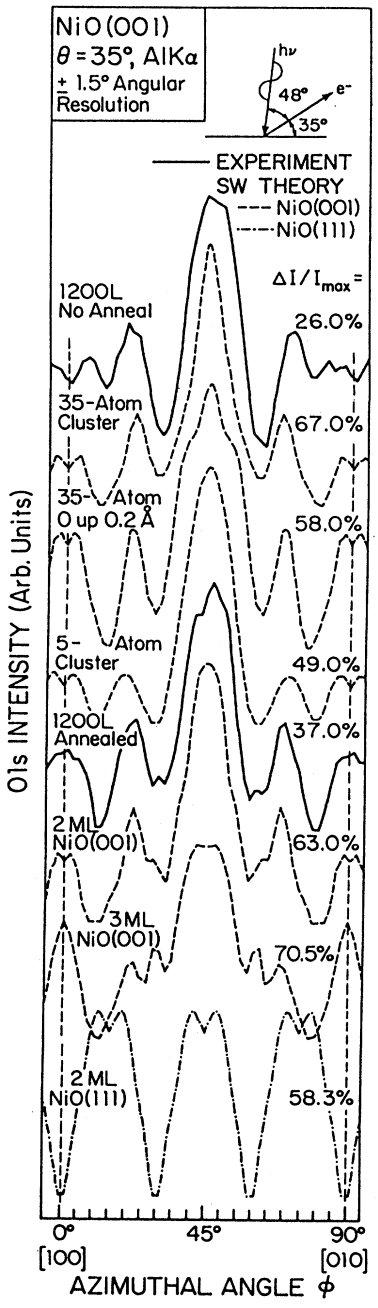

FIG. 4. Experimental azimuthal scans of O 1*s* intensity obtained with a high angular resolution of ±1.5° at $\theta=35.3°$ before and after a light anneal of the oxide are compared to the results of theoretical diffraction calculations for several clusters. The NiO(001) clusters without long-range order are indicated in Fig. 3(b) and described in the text.

bottoms of Figs. 4 and 5 are for ideal 2- and 3-ML overlayers of NiO(001) with long-range order, as well as for a sum of two domains of 2 ML of NiO(111) with long-range order that is consistent with the 12-spot ring seen before annealing. In both figures it is clear that the annealed oxide yields XPD curves that are in remarkably good agreement with those of the ideal 2 ML of NiO(001), with noticeably less agreement as to fine structure for an ideal 3 ML of NiO(001). Thus, we conclude that the annealed oxide exists as NiO(001) and that it has been well ordered in the top 2 ML by the anneal. Some disordered oxide that is not as obvious in the XPD curves is probably still present below these top 2 ML, since our surface stoichiometry suggests that another 2–3 ML of oxygen may be present after the anneal, particularly if there is thickening and island formation. This more deeply buried and strained oxide may be responsible for the lower experimental anisotropy (37%) compared to theory (63%). A prior XPD analysis of the vertical separation of the oxide layers for the annealed oxide based upon the positions of forward-scattering peaks in polar scans[4] also suggests that it is very close to the one-half of $\frac{7}{6}$ of the Ni lattice constant (a_{Ni}) which is expected if the oxide has the same $\frac{1}{6}$-expanded lattice constant in all three dimensions. This assumption has thus been used in all of the calculations reported here.

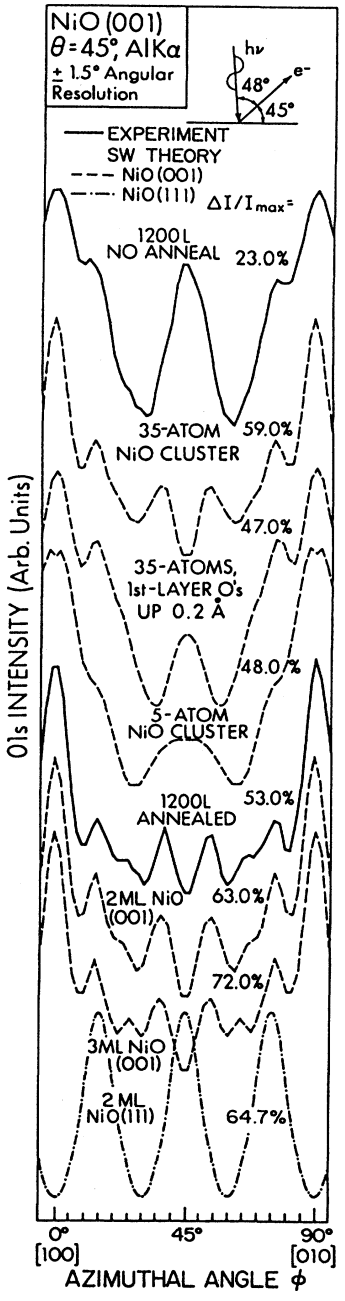

FIG. 5. Same as Fig. 4, but for $\theta=45°$.

Turning now to the ambient-temperature oxide that exhibits the superlattice structure, we have carried out several calculations to simulate some of the effects of strain and the loss of long-range order, considering the first 2–3 ML of oxide that would be most important in producing the photoelectron-diffraction pattern. In the upper portions of Figs. 4 and 5, we show theoretical calculations for three different clusters whose makeup is illustrated in Fig. 3(b).

(i) A 35-atom cluster of 2 ML of NiO(001) spanning only about two unit cells.

(ii) The same 35-atom cluster with the surface-layer O atoms moved upward by only 0.21 Å (a displacement suggested by measurements of the precise θ positions of the forward-scattering peaks in Figs. 4 and 5 from separate polar scans).

(iii) Finally a five-atom cluster that includes only the emitter in the second layer plus the four atoms nearest to the emitter along the scan directions in the second layer [as indicated more darkly in Fig. 3(b)].

In all of these calculations, we have assumed that both the vertical and lateral lattice constants of the oxide are expanded by $\frac{1}{6}$ relative to the underlying a_{Ni} to give $a_{NiO}=4.11$ Å.

In both Figs. 4 and 5 the 35-atom curve of the undistorted cluster looks rather like that of ideal 2 ML NiO(001), a result which is consistent with the known short-range sensitivity of XPD.[5] (Recall that all calculations have been made for a $\frac{1}{6}$ dilated oxide lattice.) However, there is considerable sensitivity of these curves to either a slight upward displacement of the O atoms in the 35-atom cluster or a much reduced cluster size, as shown in the second two theoretical curves in each figure. It is interesting here that either of these two cluster changes yields curves that agree better with the unannealed experimental results. Thus, although we cannot choose between these two possible structures in what may be a very strained system with a continuum of structural variations from point to point, it seems clear that our XPD results for the ambient-temperature oxide are fully consistent with the proposed strained superlattice.

We now consider the bottom theoretical curves in both Figs. 4 and 5 for two symmetry-related domains of 2 ML

of NiO(111) with long-range order, a case which might be expected to simulate whatever NiO(111) is present in domains of sufficient size and order to yield the relatively sharp (but weak) 12-spot ring in Fig. 1(a). These NiO(111) curves do not yield any major features that are in agreement with those seen in the unannealed oxide curves, and it is clear that the dominant species present is NiO(001). However, closer inspection does reveal that certain weaker features in the experimental data for the unannealed oxide may be at least partially caused by XPD from the minority NiO(111) present. For example, in Fig. 4 the experimental data for the unannealed oxide exhibit a filling in of the valleys in the NiO(001) theoretical curves at $\phi=12°$ and 78° that may be linked to the peaks at similar positions for NiO(111). In Fig. 5 the shoulders at $\phi=15°$ and 75° and the strong peak at $\phi=45°$ in the data for unannealed oxide all could contain contributions from the regular peaks for NiO(111) at the same positions. However, taking linear superpositions of the theoretical curves for unannealed NiO(001) and NiO(111) with various mixing coefficients x and $1-x$, respectively, indicates that the overall best fits to the unannealed data represent only about 5% NiO(111). The maximum amount possible is only 10%. We thus conclude that, even though some of the surface must exist in the (111) structure with sufficiently large domains to yield the relatively sharp 12-spot ring seen in fig. 1(a), the dominant species of oxide on Ni(001) is NiO(001).

Lastly, we comment briefly on the relative lattice constants exhibited by NiO in its growth on Ni(001). The lattice constant of bulk NiO in the NaCl structure is 1.184 times that of Ni. For the superlattice, we have proposed an average value of $\frac{7}{6}=1.167$ times, or a 1.7% contraction relative to bulk NiO. Thus, NiO(001) grows on Ni(001) with very nearly its normal lattice constant. For the two-domain NiO(111) structure thought to cause the 12-spot ring[9] the perfect matching of $\langle 110 \rangle$ row spacings of Ni(001) with those of the most closely spaced rows in (111) planes of NiO requires an NaCl lattice constant of 1.154 times Ni, or a 2.5% contraction relative to the bulk oxide. The amount of contraction required and thus the net energy change involved is very close for the two cases, and it is thus perhaps not surprising that they can coexist on the surface. However, the fact that the growth of NiO(001) requires less contraction may explain its statistical dominance. In comparative data for another Ni surface, Christensen *et al.*[3] find evidence for a similar sort of superlattice in LEED measurements in an early stage of high-temperature oxidation of Ni(111). Here, a NiO(001) structure beats against the underlying Ni(111) surface; however, their simulations of the LEED pattern require a 7% *expansion* of the NiO lattice relative to its bulk value that is much larger than and in the opposite direction to ours.

CONCLUSIONS

The oxidation of Ni(001) is dominated by the formation of NiO(001), which, at ambient temperature, grows in a strained lateral superlattice. This superlattice oxide is expanded in lattice constant by $\frac{1}{6}$ relative to Ni(001), as seen via extra spot splittings in LEED that have not been discussed previously. Azimuthal XPD data at high angular resolution further indicate that this oxide is highly strained, but that the first two layers can be very well ordered by a brief low-temperature anneal to approximately 250 °C. Comparisons to calculated single-scattering diffraction curves are found to yield excellent agreement for the annealed oxide. Using such theoretical curves the amount of NiO(111) present in the unannealed oxide is estimated to be 5%, and cannot be more than 10%, even though it is thought to be responsible for the presence of a 12-spot ring pattern in LEED. Both NiO(001) and NiO(111) are contracted by very nearly the same amount in lattice constant relative to bulk NiO, but NiO(001) is less so. Our total coverages of saturated oxide at 1200-L exposure are 4.3 ± 0.4 ML before annealing and 2.0–3.0 ML after annealing. The importance of both fully reaching saturation and allowing adequately for inelastic attenuation in the oxide overlayer has also been demonstrated.

Beyond these specific structural conclusions concerning the oxidation of Ni(001), we also note that this study has demonstrated for the first time a high sensitivity of XPD with resolutions of approximately $\pm1°$ to relatively subtle changes in the degree of short-range order around a given type of emitter. Thus, such measurements should be very useful in studies of the growth of various types of strained epitaxial overlayers, islands, or clusters on single-crystal substrates. Prior work on epitaxial systems using either Auger-electron diffraction or XPD (Refs. 13 and 14) has largely made use of lower-resolution data in which the principal diagnostic features are the strong forward-scattering peaks along near-neighbor directions. But the results presented here indicate that considerably more detailed structural information can be extracted from higher-resolution data which more clearly exhibit features due to higher-order interference phenomena. As one example of this kind of study, the growth of metastable crystal structures such as epitaxial fcc Fe on Cu(001) (Ref. 15) must be associated with strain and misfit dislocations, particularly for thicker layers which often tend to revert to the normal crystal structure. High-resolution XPD should be capable of studying the degree of disorder present near the surface as a function of thickness. Similarly, XPD from islands or clusters should be sensitive to both the size of the agglomeration and the degree of order within it.[16]

ACKNOWLEDGMENTS

We gratefully acknowledge the support of the U.S. National Science Foundation under Grant No. CHE-83-20200 and of the U.S. Office of Naval Research under Contract No. 00014-87-K-0512. One of us (C.R.B.) is pleased to acknowledge the Chemistry Department of the University of Hawaii for supporting a visit during which this work was initiated. Another (C.S.F.) was supported in part by the Laboratoire pour l'Utilisation du Rayonnement Electromagnétique de l'Université Paris–Sud, Orsay, France and Centre d'Etudes Nucléaires de

Saclay du Commissariat á l'Energie Atomique, Gif-sur-Yvette, France. Some of the theoretical calculations discussed here were performed at the San Diego Supercomputer Center (GA Technologies, Inc., San Diego, CA) with a grant of time from the University of Hawaii Remote User Access Center. We are also grateful to P. A. Thiel for helpful comments concerning our LEED interpretations.

---

*Present address: University of Fribourg, CH-1700 Fribourg, Switzerland.

[1]C. R. Brundle and J. Q. Broughton, in *The Chemical Physics of Solid and Heterogeneous Catalysis,* edited by D. A. King and D. P. Woodruff (Elsevier, Amsterdam, in press), Vol. 3.

[2]I. P. Batra and J. A. Baker, Phys. Rev. B **29**, 5286 (1984), and references to other studies therein.

[3]T. M. Christensen, C. Raoul, and J. M. Blakely, Appl. Surf. Sci. **26**, 408 (1986).

[4]R. Saiki, A. Kaduwela, J. Osterwalder, M. Sagurton, C. S. Fadley, and C. R. Brundle, J. Vac. Sci. Technol. A **5**, 932 (1987), and unpublished. The oxide expansion is incorrectly referred to as $\frac{1}{7}$ in this paper.

[5]C. S. Fadley, Prog. Surf. Sci. **16**, 275 (1984); Phys. Scr. **T17**, 39 (1987).

[6]R. C. White, C. S. Fadley, and R. Trehan, J. Electron Spectrosc. Relat. Phenom. **41**, 95 (1986).

[7]R. E. Connelly, C. S. Fadley, and P. J. Orders, J. Vac. Sci. Technol. A **2**, 1333 (1984). The mean free path for Ni $2p_{3/2}$ emission from Ni metal of 10.0 Å was taken from this reference, assumed to be the same in the oxide at the same energy, and then scaled as (kinetic energy)$^{1/2}$ to derive the additional O 1*s* mean free path needed for our analysis.

[8]J. J. Yeh and I. Lindau, At. Data Nucl. Data Tables **32**, 1 (1985).

[9]P. H. Holloway and J. B. Hudson, Surf. Sci. **43**, 123 (1974).

[10]D. F. Mitchell, P. B. Sewell, and M. Cohen, Surf. Sci. **61**, 355 (1976); D. F. Mitchell, P. B. Sewell, and M. Cohen, *ibid.* **69**, 310 (1977).

[11]J. W. M. Frenken *et al.*, Surf. Sci. **135**, 147 (1983).

[12]C. R. Brundle and H. Hopster, unpublished LEED and XPS results.

[13]S. A. Chambers, I. M. Vitomirov, S. B. Anderson, H. W. Chen, T. J. Wagener, and J. H. Weaver, Superlatt. Microstruct. **3**, 563 (1987).

[14]W. F. Egelhoff, Phys. Rev. B **30**, 1052 (1984); E. L. Bullock and C. S. Fadley, *ibid.* **31**, 1212 (1985); W. F. Egelhoff, Phys. Rev. Lett. **59**, 559 (1987), and references therein.

[15]D. A. Steigerwald and W. F. Egelhoff, Phys. Rev. Lett. **60**, 2558 (1988).

[16]E. L. Bullock and C. S. Fadley (unpublished).

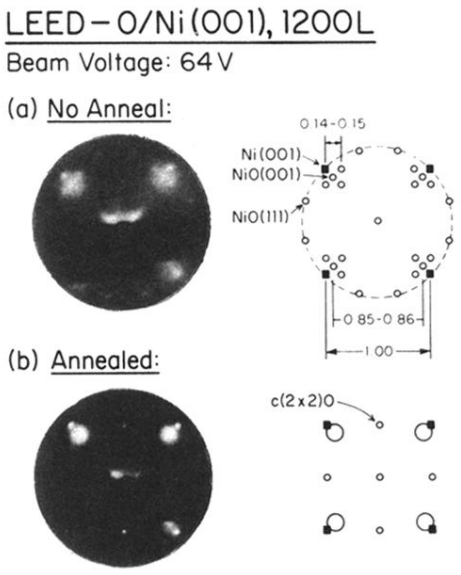

FIG. 1. (a) LEED spot pattern observed for ambient-temperature saturated oxide on Ni(001) at an incident energy of 64 eV. (The specimen holder obscures some spots from left to right across the image.) At right the positions and suggested origins of the several structures are indicated. (b) Same as (a), but after a light anneal to approximately 250 °C over about 10 min.